Characterization of Parylene-N as Flexible Substrate and Passivation Layer for Microwave and Millimeter-Wave Integrated Circuits

Hasan Sharifi, *Member, IEEE*, Rosa R. Lahiji, *Member, IEEE*, Han-Chung Lin, Peide D. Ye, *Senior Member, IEEE*, Linda P. B. Katehi, *Fellow, IEEE*, and Saeed Mohammadi, *Senior Member, IEEE*

***Abstract*—Investigation of Parylene-N (Pa-N) as a flexible substrate, multilayer dielectric material, and passivation layer for microwave and millimeter-wave integrated circuits is presented. For the first time, the electrical properties of Parylene-N have been characterized up to 60 GHz using various microstrip ring resonators and transmission lines. As a flexible substrate, Parylene-N measures a nearly invariant relative dielectric constant (ε_r) of 2.35–2.4, and a loss tangent ($\tan\delta$) of lower than 0.0006 for frequencies up to 60 GHz. Because of the above properties, as a passivation layer, Parylene-N causes insignificant modifications to the properties of underlying passive and active structures. Measurement of coplanar waveguide transmission lines before and after passivation reveals that a 5-μm Parylene-N barely changes the insertion loss (below measurement accuracy) while a 10-μm-thick Parylene-N layer increases the insertion loss by only 0.007 dB/mm (below measurement error) at 40 GHz. Ring resonators before and after a 5 or 10 μm passivation show a frequency shift of less than 0.05% or 1.51%, respectively, up to 40 GHz. The influence of Parylene-N passivation on the RF performance of GaAs MESFETs is also found to be negligible. Finally, humidity studies with dew point sensors reveal that with a 10-μm-thick passivation at 25 °C and 100% relative humidity, the MTTF is about 481.6 days. In summary, the results indicate that Parylene-N is an excellent and promising material for application at microwave and millimeter-wave frequencies.**

***Index Terms*—Dielectric characterization, microwave and millimeter-wave integrated circuit, Parylene, passivation, ring resonators.**

I. Introduction

DEMAND for low cost electronic systems with high levels of complexity has led to innovations in many application areas including integration and packaging technologies. As an example, multilayer packaging plays a critical role in achieving high performance and low cost miniaturized products for monolithic microwave integrated circuit (MMIC) applications. Hence, compatibility of the fabrication process with the MMIC technology and good radio-frequency (RF) properties, which allow the material to be used as a substrate for multilayer architecture, are important for employment in any integration schemes.

To increase the lifetime and enhance the performance of a circuit or a system, a dielectric material will be used to cover or encapsulate the entire chip. Historically, SiO_2 is among the most common materials used as passivation for high frequency circuits. It is also being used for multilayer interconnect. While the RF properties of SiO_2 make it very popular as a passivation and dielectric layer, it has a dielectric constant of 3.9, which requires a redesign for specific circuit architectures, such as those incorporating coplanar lines, and is deposited at temperatures above 300 °C which limits its post processing application. Materials such as Kapton, FR4, ceramics such as LTCC, and benzocyclobutene (BCB) are also commonly used for microwave and millimeter wave applications due to their relatively low loss characteristics. However, some of these materials need high temperature processing and find limited applicability. Recently, liquid crystal polymer (LCP) has been used as a new flexible substrate for microwave and millimeter-wave applications and has shown low relative dielectric constant (ε_r) and low loss characteristics measured by loss tangent ($\tan\delta$) [1]–[3].

Parylene, a conformal polymer coater developed by Union Carbide Corporation, is a useful alternative to LCP and other organic encapsulants. It provides excellent environmental protection as well as very good electrical properties at high frequencies. It is based on poly-para-xylylene, which is a completely linear and highly crystalline material. Parylene-C is a type of Parylene with good environmental barrier properties, which has been widely used as a passivation layer in biomedical applications and as a passivation layer on printed circuit board (PCB) [4]–[6]. Its RF and microwave characteristics have been recently reported [7]. Parylene-N is another member of the Parylene family that has been characterized at low frequencies (up to 1 MHz) and exhibits a very low dissipation factor ($\tan\delta$), a low dielectric constant, high volume resistivity as well as high dielectric strength. Parylene-C and -N have slightly different molecular structures which results in different RF and microwave properties [6], [8].Table I illustrates properties of different materials used for high-frequency applications. As demonstrated in this paper, the unique properties of Parylene-N make it an excellent candidate for monolithic microwave integrated circuit (MMIC) applications either as dielectric layer,

Manuscript received July 06, 2007; revised February 14, 2008; June 17, 2008. Current version published February 13, 2009. This work was supported by National Science Foundation under Grant ECCS 0701630. This work was recommended for publication by Associate Editor S. Dvorak upon evaluation of the reviewers comments.

H. Sharifi, R. R. Lahiji, H.-C. Lin, P. D. Ye, and S. Mohammadi are with the Birck Nanotechnology Center, Purdue University, West Lafayette, IN 47907 USA.

L. P. B. Katehi is with the Department of Electrical and Computer Engineering University of Illinois, Urbana-Champaign, IL 61820 USA.

Color versions of one or more of the figures in this paper are available online at http://ieeexplore.ieee.org.

Digital Object Identifier 10.1109/TADVP.2008.2006760

TABLE I
SUMMARY OF PROPERTIES OF DIFFERENT MATERIAL

	SiO_2	Kapton [3][9] Polyimide	FR4 [10]	LTCC [10]	LCP [1]	BCB [11]	Parylene-C [6] [7]	Parylene-N [6] and this paper
Application	M[1], E[2]	M[1], E[2], F[3]	M[1], F[3]	M[1], F[3]	M[1], F[3]	M[1], E[2], F[3]	M[1], E[2], F[3]	M[1], E[2], F[3]
Dielectric constant (ε_r)	3.9 @ 1MHz	3.4-3.5 @ 1KHz	4-5 (<10 GHz)	5.7-9.1 (<12 GHz)	3.16 (<110 GHz)	2.5 @ 10 GHz	2.95 @ 1MHz	2.4 (<60 GHz)
Loss tangent ($\tan\delta$)	2×10^{-5} @ 1MHz	$25-35\times10^{-4}$ @ 1KHz	25×10^{-3} (<10 GHz)	$12-63\times10^{-4}$ (<12 GHz)	4×10^{-3} (<110 GHz)	2×10^{-3} @ 10 GHz	0.002 <60 GHz)	6×10^{-4} <60 GHz)
Volume Resistivity [Ω-cm]	$>10^{18}$	1.5×10^{17}	8×10^{13}	1×10^{12}	5.3×10^{15}	1×10^{19}	8.8×10^{16}	1.4×10^{17}
Melting Point [°C]	> 1500	400	120-210 [Tg]	> 500	290	350 [Tg]	290	420
Water Absorption (% after 24hrs)	0	0.4-2.5	0.25	negligible	< 0.1	< 0.2	< 0.1	< 0.1
Linear Coeff. of Thermal Expan. [ppm/C]	0.5	20	17 in X &Y, 175 in Z axes	5.8-8	17	42	35	69
Coeff. of Thermal Conductivity [W/mK]	1.4	0.12	0.3	2- 4.4	0.2	0.3	0.084	0.126

(1) M: Multi-layer interconnect
(2) E: Encapsulant
(3) F= Flexible substrate

passivation layer, or even a flexible substrate. In this work, for the first time, we have characterized high-frequency properties of Parylene-N as a flexible microwave substrate, and a dielectric/passivation layer from 1 to 60 GHz.

Microstrip ring resonators of different diameters and coplanar waveguide transmission lines (CPWs) have been used for this characterization. Transmission line losses across the desired frequency range provide a design guide for this material. Parylene-N as an encapsulant has also been investigated through its moisture absorption properties. The result of this investigation gives a thorough understanding of Parylene-N properties and its performance in comparison to other organic and inorganic materials for high-frequency applications. In the following section, the deposition process and properties of Parylene-N as made available by its manufacturer are reviewed [6]. In Section III, a set of test structures is designed, fabricated, and measured to assess the RF and microwave properties of Parylene-N and demonstrate its applicability as a flexible substrate and a dielectric layer. Section IV presents the performance of Parylene-N as an encapsulant. The performances of multiple active and passive test structures before and after passivation with Parylene-N are demonstrated and the test setup and measurement results for humidity analysis are reported. Finally, a summary of our findings are presented in Section V.

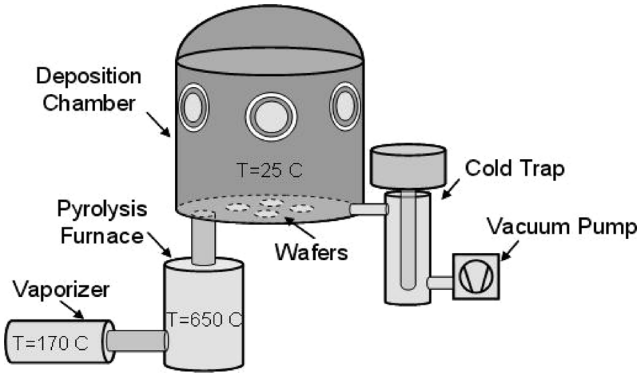

Fig. 1. Parylene-N CVD system.

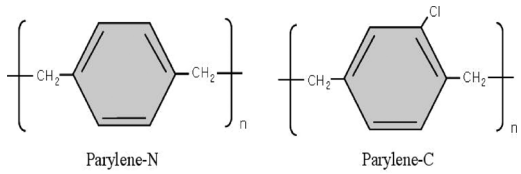

Fig. 2. Chemical structure of (a) Parylene-N and (b) Parylene-C.

II. Deposition Process and Properties of Parylene-N

Parylene-N is commercially available in a powdered dimer form. Deposition occurs at the molecular level as the dimer converts to a polymer film at room temperature under a low pressure environment (~ 60 mTorr) in a chemical vapor deposition (CVD) machine [6], as shown in Fig. 1. Similar to any vacuum system, a mechanical pump and associated protective traps are required for this system. The deposition process consists of three steps. First, the solid Parylene-N dimer is vaporized at a temperature of 120 °C–170 °C. Then the gas dimer is decomposed to monomer gas using a furnace at a temperature of 650 °C. Finally, the monomer gas enters in the deposition chamber where it spontaneously polymerizes on the substrate at room temperature. The deposition thickness can be easily controlled by the amount of the raw dimer placed in the vaporizer chamber.

The ability to deposit Parylene-N at room temperature makes it a very desirable material for postprocessing fabrication as compared to other inorganic and organic materials such as SiO_2, polyimide, and benzocyclobutene (BCB), where the deposition or curing occurs at high temperatures. Parylene-N is an excellent choice for coating heat sensitive circuits or devices with low thermal budgets. In addition, during the polymerization process Parylene-N does not shrink. Due to its greater molecular activity in the monomer state when compared with Parylene-C, Parylene-N has the highest penetrating power resulting in a uniform step coverage and pinhole-free film. Fig. 2 depicts the chemical architecture of Parylene-N and -C. As seen from the figure, Parylene-C has a single Chlorine atom on the benzene ring, while Parylene-N has a more symmetric structure. The halogen-free structure of Parylene-N is another advantage comparing to –C. In terms of deposition rate, Parylene-C has a greater rate (5μm/h) than –N (0.75 μm/h).

According to Table I, Parylene-N has better electrical properties compared to Parylene-C, however it has a higher coefficient of thermal expansion (CTE). CTE mismatch causes shear strain or stress and reduces thermal cycling lifetime. In terms of water absorption both demonstrate similar low moisture absorption properties. Parylene-N melts at 420 °C while the melting point of Parylene-C is 290 °C. Both materials are chemically stable, biocompatible, and optically transparent.

III. Parylene-N as a Microwave Substrate

Relative dielectric constant (ε_r) and loss tangent ($\tan\delta$) are the two most important dielectric properties of a material used for high frequencies. These two parameters determine the electrical properties of passive components realized on these materials. For instance, the characteristic impedance of a transmission line depends on the dielectric constant of the substrate while its quality factor is a function of the loss tangent. Therefore, it is possible to determine the material's ε_r and $\tan\delta$ from measuring properties of transmission lines of different lengths realized on the substrate understudy. For frequencies below 100 MHz, an impedance technique is used to determine ε_r and $\tan\delta$, whereby using a circular capacitor and measuring its impedance one can extract the electrical properties of this substrate. However, for measurements performed at higher frequencies, fabricating an accurate small capacitance and measuring its impedance is relatively hard. On the other hand, a resonant structure such as a microstrip-ring or a line-resonator can be fabricated and measured with high accuracy to determine the dielectric properties of the substrate. In this paper, the microstrip-ring resonator method is used due to its higher accuracy compared to that of the microstrip line resonator [1], [2].

To conduct our experiment, we started with a silicon wafer which has metallization on top acting as a backside metallization for the test structures on Parylene substrate. Then, we deposited two different thicknesses of Parylene-N (40 and 60 μm) using the CVD system shown in Fig. 1. Standard lithography and wet etching techniques were used to pattern a 4-μm-thick evaporated aluminum metal layer to form ring resonators with different thickness and diameter and 50-Ω coplanar waveguide (CPW) transmission lines with different lengths. Thick Al is used to ensure that conductive losses including the skin effect play no major role in the measurements. An adhesion promoter (A-174) from specialty coating systems (SCS) is used in order to improve the adhesion between Parylene-N and the aluminum metal patterns. A mixture of isopropyl alcohol (IPA): deionized water (DI): Silane A-174 (100:100:1) acts as surface treatment in order to improve adhesion. The samples are submerged in the prepared solution for 30 min and finally air dried before the aluminum deposition [6]. This will create only a single monolayer of the adhesion promoter on the surface. Hence, this surface treatment dose not influence the RF properties of the circuits.

Fig. 3 shows the layout of a ring resonator and the fabricated structures on the flexible Parylene-N substrate. Both Momentum from Advanced Design Systems (ADS 2005A) and Ansoft HFSS were used to perform electromagnetic simulations of

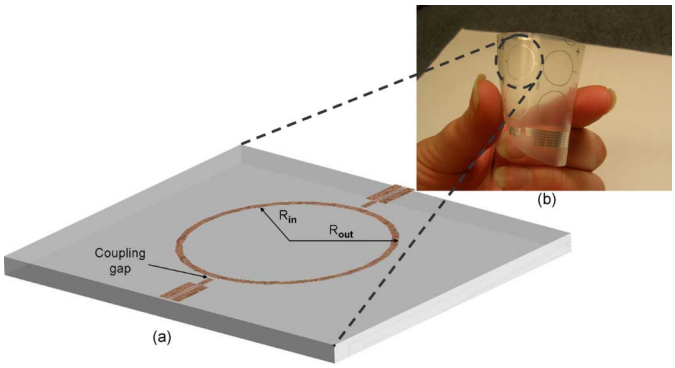

Fig. 3. (a) Layout of the designed ring resonator. (b) Fabricated structures on the flexible Parylene N substrate.

the ring resonators. The designs included two different mean radii (3 and 6 mm) with the width of $W = 200$ μm. A coupling gap size of 40 μm provided weak coupling in order to prevent loading the ring and causing numerical errors in computing the resonant frequencies and hence the extracted dielectric constant [12]. Resonances were established at frequencies where the mean circumference of the ring was equal to integer multiples of the guided wavelength ($n\lambda_g = 2\pi r$) [12], [13]. Hence

$$f_n = \frac{nc}{2\pi r\sqrt{\varepsilon_{\text{eff}}}} \tag{1}$$

where c is the speed of light in vacuum, n is the number of half wavelengths, ε_{eff} is the effective dielectric constant, and r is the mean radius (average of the inner and outer radii, R_{in} and R_{out}). By determining the peak frequencies where resonances happen, the relative dielectric constant of Parylene-N versus frequency was derived using the effective dielectric constant and the physical dimensions of the microstrip ring-resonators [2] as shown in the following equations:

$$\varepsilon_r = \frac{2.\varepsilon_{\text{eff}} + M - 1}{M + 1} \tag{2}$$

where $M = (1 + 12h/W_{\text{eff}})^{-1/2}$, W_{eff} is the effective width of the line defined as $W_{\text{eff}} = W + (1.25t/\pi)[1 + \ln(2h/t)]$. W and t are the physical width of the line and the metal thickness, respectively, and h is the thickness of the Parylene-N substrate.

Total loss including conductor loss, dielectric loss and radiation loss can be determined by measuring the bandwidth and insertion loss at each resonance frequency [12] using

$$\alpha_{\text{total}} = \frac{27.3}{\left(\frac{f_0}{BW_{-3\text{ dB}}}\right)\lambda_g} \times (1 - 10^{-L/20}) \tag{3}$$

where L is the insertion loss in decibels at each resonance frequency, and $\lambda_g = c/f\sqrt{\varepsilon_{\text{eff}}}$. The dielectric loss is calculated as $\alpha_d = \alpha_{\text{total}} - \alpha_c$, where α_c is the conductor loss. By knowing the dielectric loss, loss tangent ($\tan\delta$) is extracted according to the following equation:

$$\tan\delta = \frac{\alpha_d \varepsilon_{\text{eff}}}{0.9094\varepsilon_r f}. \tag{4}$$

The conductor loss was calculated using the theoretical equation provided by [14]. Regarding radiation loss, the only source of radiation is generated by the open-ended microstrip feeding lines since radiation from the ring resonators is negligible due to geometrical continuity of the ring. Due to inherent inaccuracies of the theoretical models, we did not extract and subtract the radiation loss from the total loss due to introduced numerical errors which are comparable to the calculated values of the electrical parameters.

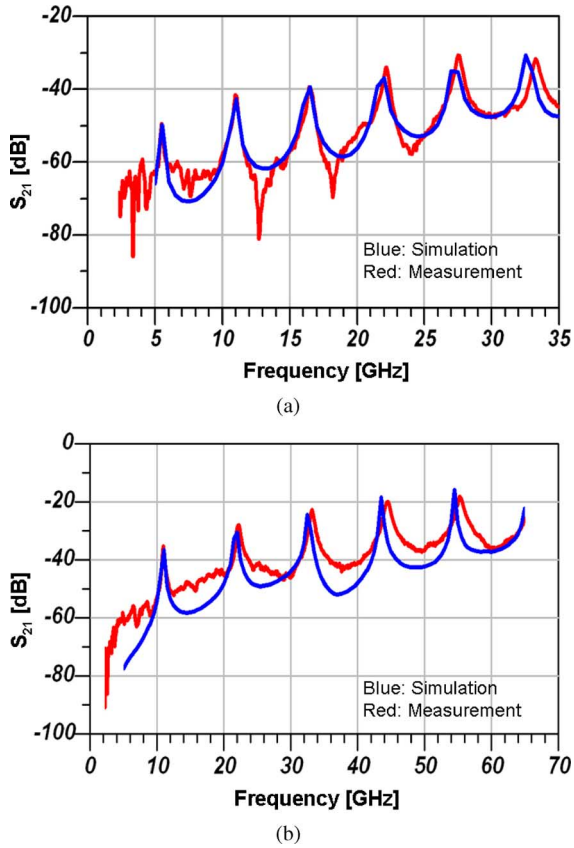

Fig. 4. Simulation and measurement of insertion loss for (a) 6-mm and b) 3-mm ring resonator.

For improved accuracy, RF characterization was performed using the Agilent 8510XF vector network analyzer at two different frequency ranges. The range from 1 to 65 GHz range was used for the 3-mm ring while the range from 1 to 35 GHz range was used for the 6-mm ring resonator. In order to eliminate the effects of the feeding sections, a TRL calibration technique with four different delay lines as well as an open, and a short was used. Fig. 4(a) and (b) illustrates simulated and measured values of S_{21} of the 6- and 3-mm ring resonators, respectively. The simulations have been done by using $\varepsilon_r = 2.4$ and loss tangent of 0.0006. As the results show the simulated and measured insertion losses match fairly well.

The values of ε_{eff} and ε_r are calculated using (1) and (2). The extracted ε_r values from two 3-mm-radius and two 6-mm-radius devices are illustrated in Fig. 5. As the figure shows, the average value of the dielectric constant (ε_r) of Parylene-N is between 2.35 and 2.4 from 1 to 60 GHz. The dielectric constant varies by less than 2.1% over the entire measured frequency range.

From the above measurements, the loss tangent of Parylene-N is extracted according to (4) and it is plotted as a function of frequency as shown in Fig. 6.

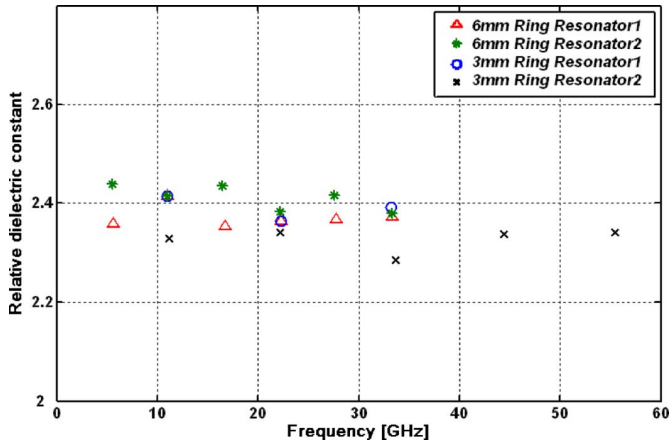

Fig. 5. Relative dielectric constant of Parylene-N extracted from measurements.

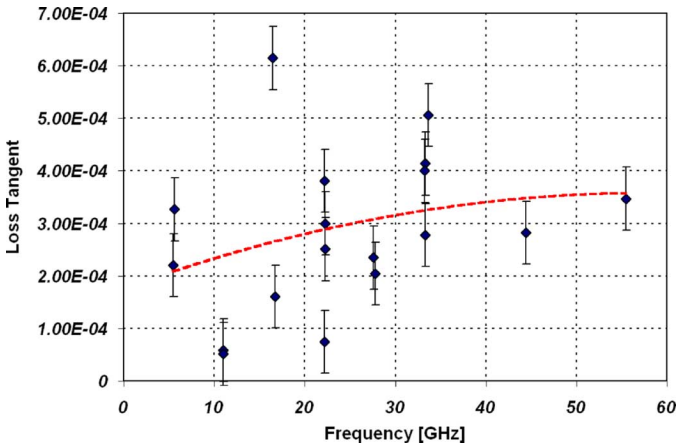

Fig. 6. Loss tangent of Parylene-N extracted from measurements.

The loss tangent values are mostly between 0.0002 and 0.0004. The dashed line is the best fitted forth-degree polynomial to the measured data. When comparing to LCP and other inorganic and organic materials, Parylene-N has the lowest dielectric constant and the lowest loss tangent which, when considering its room temperature process, makes it an ideal candidate for MMIC applications.

IV. Parylene-N as an Encapsulant

Passivation layers used as encapsulants should have low loss and low dielectric constant in order to minimize the impact on the RF performance of the encapsulated circuits. To study the properties of Parylene-N as a passivation layer, we have utilized a glass wafer as a substrate for passive structures and a GaAs wafer as a substrate for active devices. The glass wafer has a thickness of 500 μm with the dielectric constant of 7.2 and loss tangent of 0.006. Through a combination of lithography and liftoff processes, a 4-μm–thick evaporated Aluminum layer is patterned to form passive microwave structures, namely CPW transmission lines and ring resonators. The chuck is used in lieu of backside metallization. An adhesion promoter (A-174) is used in order to improve the adhesion between Parylene-N and the substrate. A thin layer of Parylene-N with thicknesses of 5 or 10 μm is deposited across the sample to form a uniform cover over the substrate with a peak-to-valley roughness of less than 0.02 μm as measured across the wafers. To complete the process, Parylene-N is etched through by oxygen plasma using the Reactive Ion Etching (RIE) technique to form the opening windows for the probe pads. The microwave properties of these passive structures are measured and comparisons are made for the same structures before and after passivation with two different passivation thicknesses (5 μm and 10 μm). While CPW transmission lines with different lengths have been used to accurately estimate the additional loss per millimeter length introduced by the passivation layer, ring-resonator structures are used to identify the effect of the dielectric constant of the passivation layer on the circuits. Choosing ring resonators with a radius $r = 6$ mm on the glass wafer results in peak resonances that are multiples of 3.83 GHz, while $r = 3$ mm results in resonances at integer multiples of 7.66 GHz.

In order to measure the S-parameters of the weak coupled resonators, microstrip to CPW transitions were added at both ends. For the CPW transmission lines feeding the ring resonators, a high impedance of about 60 Ω (higher than nominal 50-Ω lines) was selected in order to reduce the dispersion that is common in microstrip configurations of ring resonators [15]. The dimensions of the CPW line were designed to be 65 μm – 30 μm – 300 μm as signal (S)- gap (Gap)- finite ground (FG), respectively.

We have also conducted an experiment to study the effect of Parylene-N as a passivation layer on active devices. For this experiment we have chosen GaAs MESFET transistors without any original passivation layer. A layer of 5-μm–thick Parylene-N is deposited all across the sample to form a uniform cover over the entire chip. The fabricated ring resonators on glass wafer as well as GaAs MESFET transistors with and without passivation are measured from 1 to 40 GHz using the 8510XF network analyzer with TRL calibration. The results for the three cases (structures before passivation and after passivation with 5 and 10 μm of Parylene-N) for ring resonators are depicted in Fig. 7.

As observed from the measured data the maximum shift in frequency up to 40 GHz is less than 1.51% for the 10-μm passivation layer, while the shift is less than 0.05% for the 5 μm thickness. According to a recent report by Karnfelt *et al.* [7] a 5-μm Parylene-C coating causes a frequency shift of about 0.4% at 40 GHz. This value is relatively higher than what is observed with Parylene-N. This is due to the fact that the dielectric constant of Parylene-N is lower than Paralyne-C and remains constant with respect to frequency. The transmission response ($S_{21} = S_{12}$) of the CPW lines with various lengths printed on the three different samples is also measured.Fig. 8 shows the loss per millimeter (dB/mm) of a CPW transmission line with a length of 1 mm on the glass substrate. We have three samples: 0, 5, and 10 μm of Parylene-N as a passivation layer. A measured insertion loss of better than 0.255 dB/mm is observed up to 40 GHz for both the lines without the passivation and with 5-μm-thick passivation. The insertion loss for the 10-μm-thick passivation is better than 0.262 dB/mm indicating an increase of only 0.007 dB/mm over the nonpassivated structure. These measurements make it clear that Parylene-N when used as passivation layer does not have a significant influence on the insertion loss of CPW transmission lines.

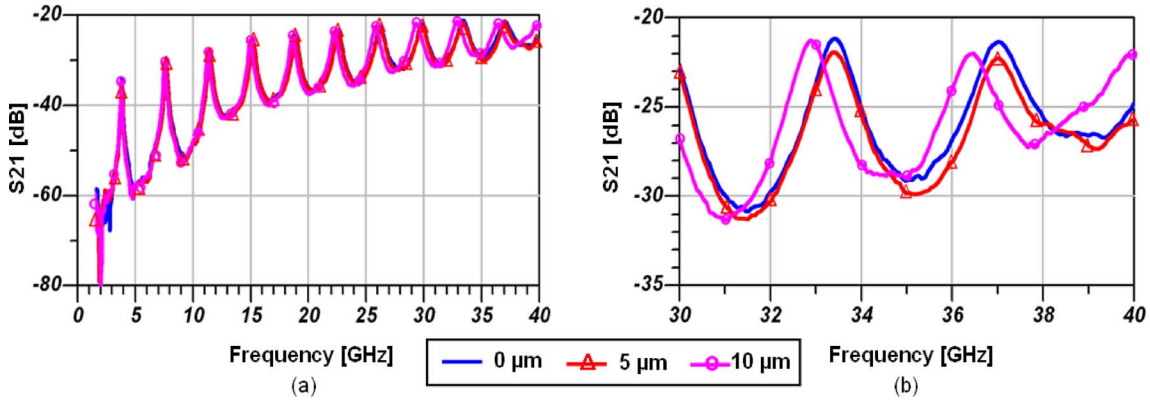

Fig. 7. (a) The measured transmission coefficient of 6-mm ring resonator with 0, 5, and 10 μm of Parylene-N passivation layer. (b) Closer look at 30–40 GHz range of graph (a).

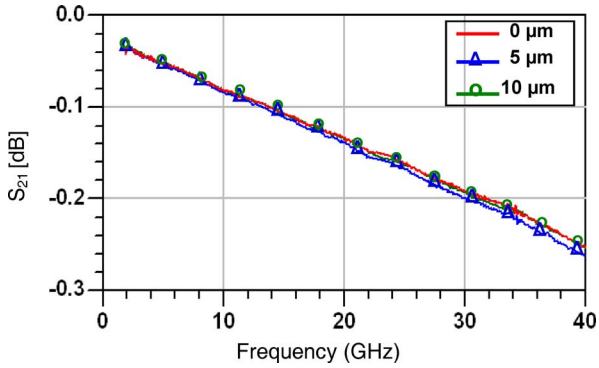

Fig. 8. The loss per millimeter (dB/mm) of a CPW transmission line with a length of 1 mm on the glass substrate with 0, 5, and 10 μm of Parylene-N as a passivation layer.

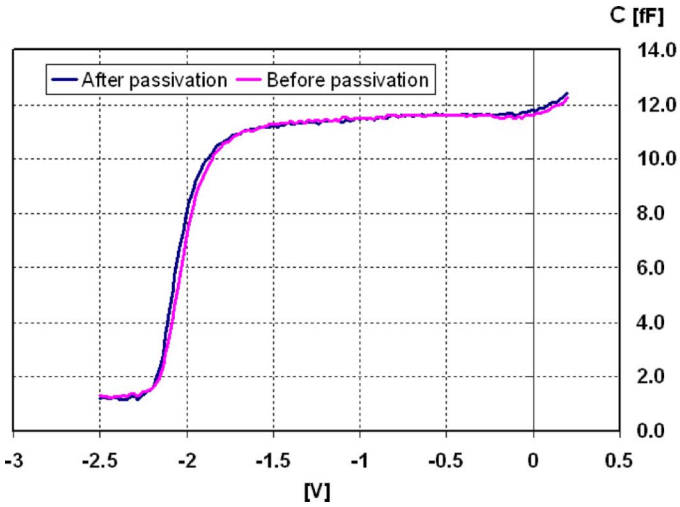

Fig. 9. C-V measurements of GaAs MESFET transistors before and after passivation.

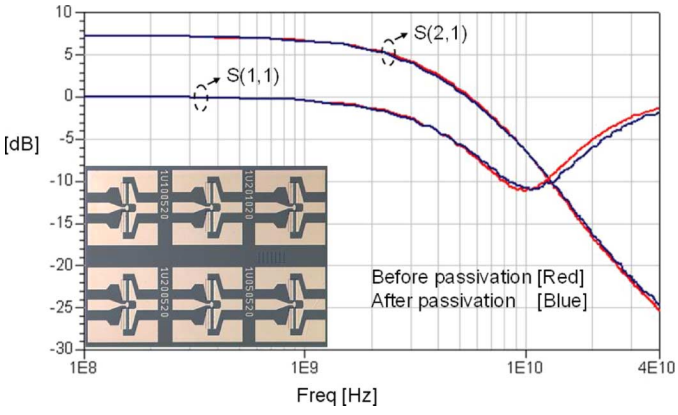

Fig. 10. S-parameter measurements of GaAs MESFET transistors before and after passivation. (The inset shows the fabricated devices.)

Figs. 9 and 10 illustrates C-V measurements and high frequency S-parameter measurements of GaAs MESFET transistors before and after a 5-μm passivation, respectively. As observed from the measured data, the passivation layer has an insignificant influence on the C-V measurement and threshold voltage as well as on the high frequency performance of the GaAs MESFETs.

In order to test and characterize Parylene-N as an encapsulant, we have also performed accelerated reliability tests to find the effect of water absorption on the package lifetime. Ideally, the reliability tests should be conducted in the real environment in which the package is operating. However, measuring in a real environment results in prolonged characterization times and increased cost. As a result, accelerated reliability tests are usually carried out at much higher stress conditions, which intensify and thus accelerate failure [16], [17]. In order to estimate the package lifetime, the Weibull probability distribution function (pdf) as shown in (5) has been used

$$f(t) = \frac{\beta}{\lambda}\left(\frac{t}{\lambda}\right)^{(\beta-1)} e^{-(t/\lambda)^{\beta}} \tag{5}$$

where t is the time, λ is the lifetime parameter, related to the mean time to failure (MTTF), and β is the shape parameter which determines how the failure frequency is distributed around the average lifetime. The cumulative distribution function $F(t)$ is given by

$$F(t) = 1 - e^{-(t/1\lambda)^{\beta}}. \tag{6}$$

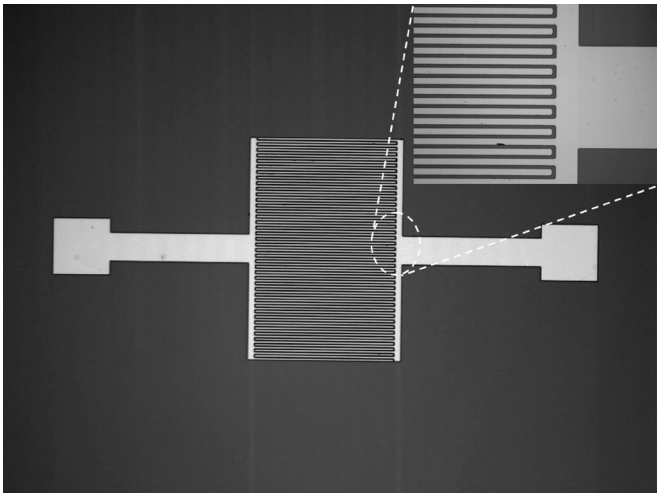

Fig. 11. Fabricated dew-point sensor.

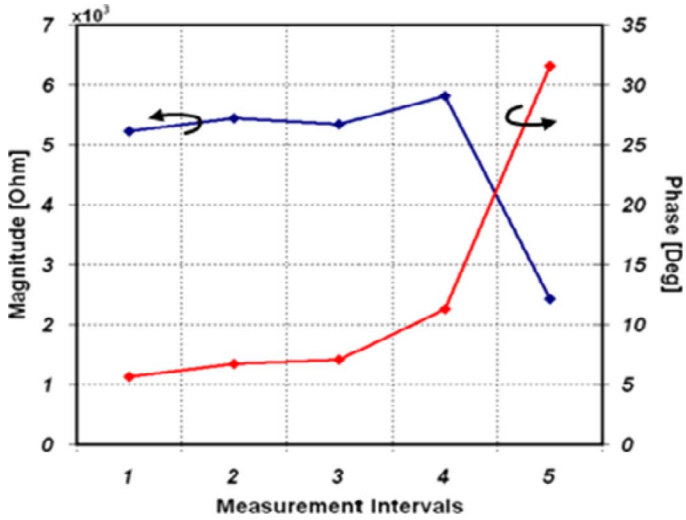

Fig. 12. Measured impedance variation of a dew point sensor during accelerated testing.

The reliability tests start with N samples at $t_0 = 0$. After time t_1, n samples are failed and $(N - n)$ samples are still functional. After time t_2, M more samples fail and $(N-n-M)$ are still functional and so on. This failure procedure continues until enough data can be collected for the estimation of the Weibull distribution parameters. In order to estimate λ and β, the cumulative Weibull distribution function is transformed so that it appears in the familiar form of a straight line: $(Y = mX + b)$ as shown below

$$Y = m\,X + b$$

$$\ln\left(\ln\left(\frac{1}{1-F(t)}\right)\right) = \beta\ln(t) - \beta\ln(\lambda)$$

where $\mathrm{m} = \beta$, $\mathrm{X} = \ln(\mathrm{t})$, and $\mathrm{b} = -\beta\ln(\lambda)$. Using the linear regression analysis, one can find m and b or β and λ.

Then, the MTTF is evaluated from

$$\mathrm{MTTF} = \lambda \times \Gamma\left(1 + \frac{1}{\beta}\right) \tag{7}$$

where Γ is the gamma function.

Once the accelerated tests are performed and the Weibull distribution parameters are extracted from the linear regression method, the MTTF can be calculated from (7) using the Γ function. There are several analytical models that are commonly used for actual product life estimation at normal conditions. One of these models is the Peck's Temperature–Humidity model [18], [19]. Using this model, the acceleration factor (AF) is defined as the ratio of the actual time to failure under normal conditions to that under accelerated conditions as follows:

$$\mathrm{AF} = \frac{(\mathrm{RH}^{-n}\exp^{\Delta E_0/kT})\mathrm{normal}}{(\mathrm{RH}^{-n}\exp^{\Delta E_0/kT})\mathrm{accelerated}} \tag{8}$$

where RH is the relative humidity, T is the absolute temperature, and k is the Boltzman constant. According to the Peck's model, we have chosen $\Delta E_0 = 0.9$ as the activation energy and $n = 3$ [16].

In order to test and find the lifetime of an encapsulant package, we have designed and fabricated a number of dew-point sensors on silicon wafers, as shown in Fig. 11 [20]–[22]. The design of the dew point sensor is usually based on an interdigitated capacitive structure, whose impedance value strongly depends on the water drops condensed on the surface of the capacitive electrodes.

The fabrication of the sensors is performed by depositing Ti/Au metallization and patterning it using a liftoff process with spacing between the lines of 5 μm. After the liftoff process, Parylene-N is deposited on the sensors and an accelerated testing in 100% relative humidity and 70 °C is performed where the impedance of the sensors is measured in different time intervals. The concept of failure is based on a drastic change in the impedance values during the accelerated test period. Once moisture condenses on the surface of the electrodes, the magnitude of the impedance decreases sharply while a sudden increase in phase is observed. Fig. 12 demonstrates the measurement results from one sensor.

The package lifetime is characterized by measuring an impedance change of 49 encapsulated dew point sensors while they are immersed in a hot water bath (100% RH) at 70 °C. After completion of the failure test over time, the data are fitted with a Weibull cumulative distribution function (cdf) using least square analysis. Based on the extracted data, the life and shape parameter are derived to be $\beta = 0.98$, $\lambda = 115.5$, respectively, and the accelerated MTTF is evaluated as 116.4 h. Using the Peck's model, the acceleration factor is 99.3 at 25 °C and 100% RH, thus the MTTF in such conditions will be 481.6 days. According to a recent report by Liang *et al.* [22], a life time of 300 days has been achieved for hermetic encapsulation for MEMS structures. The package life time can be increased by utilizing a thicker passivation layer. The estimated life time versus testing temperature is shown in Fig. 13.

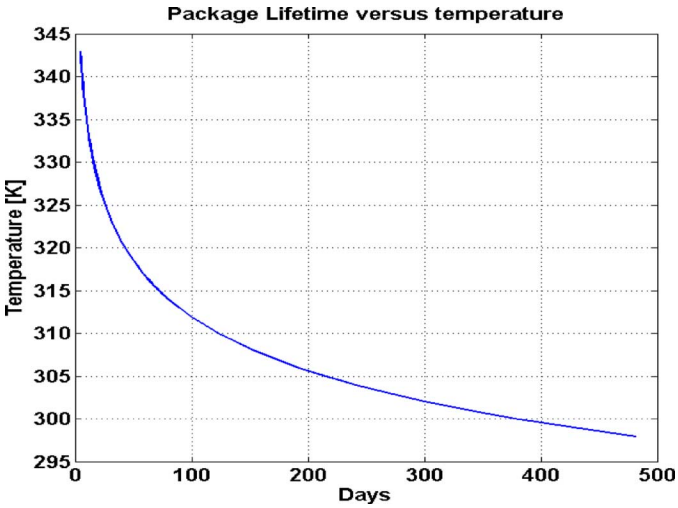

Fig. 13. Package lifetime versus testing temperature.

V. Conclusion

Parylene-N has demonstrated excellent RF, electrical, and mechanical properties. Due to its room temperature deposition and its high compatibility with modern MMICs fabrication processes and guidelines, it is a promising candidate for high-frequency applications. For the first time, the dielectric properties of Parylene-N and its performance on various structures have been characterized up to 65 GHz. Using the ring resonator method, the results show a frequency independent dielectric constant (ε_r) of 2.35–2.4 and a very low loss tangent ($\tan\delta$), less than 0.0006. Comparing to LCP and other inorganic and organic materials, Parylene-N has the lowest dielectric constant and the lowest loss tangent which makes it an ideal candidate for MMIC applications. In this work by measuring different CPW lines and ring resonators on a glass wafer as well as GaAs MESFET transistors, the effect of Parylene-N as a passivation layer on passive and active components has been studied. As the measurements reveal, this material demonstrates an increase of 0.007 dB/mm insertion loss and a frequency shift of less than 1.51% up to 40 GHz, for 10 μm of coating; properties that make this material ideal for high-frequency applications. On the other hand a 5-μm-thick coating does not influence the insertion loss while the observed frequency shift is less than 0.05%. The influence of Parylene-N on the RF performance of active components such as the GaAs MESFET transistors has also been studied and shows negligible effect. Finally, humidity studies with dew point sensors show that with a 10-μm-thick passivation at 25 failure (MTTF) is about 481.6 days. Hence Parylene-N is a strong candidate as a flexible substrate and dielectric multilayer as well as an encapsulant for MMIC applications reported to date.

Acknowledgment

The authors would like to thank Birck Nanotechnology staff members as well as the Specialty Coating Systems Company for their helpful correspondence regarding our processing.

References

[1] D. C. Thompson, O. Tantot, H. Jallageas, G. E. Ponchak, M. M. Tentzeris, and J. Papapolymerou, "Characterization of liquid crystal polymer (LCP) material and transmission lines on LCP substrates from 30 to 110 GHz," *IEEE Trans. Microwave Theory Tech.*, vol. 52, no. 4, pp. 1343–1352, Apr. 2004.

[2] G. Zou, H. Gronqvist, J. P. Starski, and J. Liu, "Characterization of liquid crystal polymer for high frequency system-in-a-package applications," *IEEE Trans. Adv. Packag.*, vol. 25, no. 4, pp. 503–508, Nov. 2002.

[3] Z. Wei and A. Pham, "Liquid crystal polymer for microwave/millimeter wave multi-layer packaging," in *IEEE MTT-S Dig,*, Jun. 2003, vol. 3, pp. 2273–2276.

[4] R. Olson, "A protective conformal coating for hybrid circuits," *Hybrid Circuit Technol.*, 1985.

[5] T. Stieglitz, "Biomedical micro implants for sensory and motor neuroprostheses," in *IEEE Int. Symp. Circuits Syst.*, May 2006, pp. 2189–2192.

[6] Specialty Coating Systems Co. (SCS). Indianapolis, IN.

[7] C. Karnfelt, C. Tegnander, J. Rudnicki, J. P. Starski, and A. Emrich, "Investigation of Parylene-C on the performance of millimeter-wave circuits," *IEEE Trans. Microwave Theory Tech.*, vol. 54, no. 8, pp. 3417–3425, Aug. 2006.

[8] R. Callahan, G. Raupp, and S. Beaudoin, "Etching Parylene-N using a remote oxygen microwave plasma," *J. Vac. Sci. Technol. B.*, vol. 20, no. 5, pp. 1870–1877, Sep. 2002.

[9] [Online]. Available: http://www.kapton-dupont.com*HYPERTEXT*,

[10] L. Devlin, G. Pearson, and J. Pittock, "RF and microwave component development in LTCC," in *IMAPS Nordic 38th Annu. Conf.*, Sep. 2001, pp. 96–110.

[11] [Online]. Available: http://www.dow.com

[12] K. Chang and L. Hsieh, *Microwave Ring Circuits and Related Structures*. New York: Wiley, 2004.

[13] L. Hsieh and K. Chang, "Equivalent lumped elements G, L, C, and unloaded Q's of closed- and open-loop ring resonators," *IEEE Trans. Microwave Theory Tech.*, vol. 50, no. 2, pp. 453–460, Feb. 2004.

[14] K. C. Gupta, R. Garg, I. Bahl, and P. Bhartia, *Microstrip Lines and Slotlines*. Norwood, MA: Artech House, 1996.

[15] J. Frey and K. Bhasin, *Microwave Integrated Circuits*. Norwood, MA: Artech House, 1985.

[16] A. Magomenos and L. P. B. Katehi, "Fabrication and accelerated hermeticity testing of an on-wafer package for RF MEMS," *IEEE Trans. Microwave Theory Tech.*, vol. 52, no. 6, pp. 1626–1636, Jun. 2004.

[17] R. R. Tummala, E. J. Rymaszewski, and A. G. Klopfenstein, *Microelectronics Packaging Handbook*. New York: Thompson, 1997.

[18] S. Peck, "Comprehensive model for humidity testing correlation," in *24th Annu. Proc. Reliabil. Phys. Symp.*, Anaheim, CA, Apr. 1986, pp. 44–50.

[19] D. Halliberg and S. Peck, "Recent humidity accelerations a base for testing standards," *Qual. Reliab. Eng. Int.*, vol. 7, no. 3, pp. 169–180, 1991.

[20] M. G. Kovac, D. Chleck, and P. Goodman, "A new moisture sensor for in-situ monitoring of sealed package," in *Proc. Int. Reliabil. Phys. Symp.*, 1977, pp. 85–91.

[21] B. Ziaie, J. A. Von Arx, M. Dokmeci, and K. Najafi, "A hermetic glass-silicon micropackage with high-density on-chip feedthroughs for sensors and actuators," *J. Microelectromech. Syst.*, vol. 5, pp. 166–179, Sep. 1996.

[22] Z. Liang, Y. Cheng, W. Hsu, and Y. Lee, "A wafer-level hermetic encapsulation for MEMS manufacture application," *IEEE Trans. Adv. Packag.*, vol. 29, no. 3, pp. 513–519, Aug. 2006.

Hasan Sharifi (S'05–M'06) received the Ph.D. degree in electrical engineering in the areas of microelectronics and nanotechnology from Purdue University, West Lafayette, IN, in 2007.

He is currently a research staff member at Birck Nanotechnology Center, Purdue University, West Lafayette, IN. His research interests are in the areas of RF and microwave devices and circuit, 3-D integration and advanced microelectronic packaging, nanoelectronics, and nanofabrication technologies.

Rosa R. Lahiji (S'97–M'07) received the B.S. degree in electrical engineering from University of Tehran, Tehran, Iran, in 2000, and the M.S. degree from University of Michigan, Ann Arbor, in 2003. She is currently working toward the Ph.D. degree in electrical engineering at the Birck Nanotechnology Center, Purdue University, West Lafayette, IN.

She is currently a research assistant at Purdue University, West Lafayette, IN. Her research interests include CMOS RF and microwave circuits design, 3-D integration of RF and microwave circuits and systems, and advanced packaging techniques using polymer-based material.

Han-Chung Lin was born in Taipei, Taiwan, in 1976. He received the B.S. degree in electrical engineering from National Taiwan University, Taipei, Taiwan, in 1999, and the M.S. degree in electrical engineering from Purdue University, West Lafayette, IN, in 2000, where he is currently working toward the Ph.D. degree, working on GaAs MOSFET with atomic layer deposited high-κ dielectrics, at the School of Electrical and Computer Engineering.

Between 2000 and 2003, he was Research Engineer at Bell Labs-Lucent Technologies.

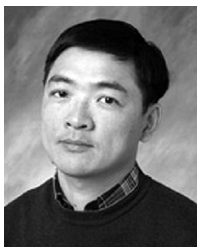

Peide D. Ye (M'00–SM'04) was born in Suzhou, China, in 1966. He received the B.S. degree in electrical engineering from Fudan University, Shanghai, China, in 1988, and the Ph.D. degree in physics from the Max-Planck Institute for Solid State Research, Stuttgart, Germany, in 1996.

Between 1996 and 2000, he was a Postdoctoral Researcher at NTT Basic Research Laboratories, Japan, and the National High Magnetic Field Laboratory/ Princeton University. Between 2001 and 2002, he was Member of Technical Staff at Bell Labs Lucent Technologies and Agere Systems, and became a Senior Member of Technical Staff in 2003. Since January 2005, he has been an Associate Professor of Electrical and Computer Engineering at Purdue University, West Lafayette, IN, working on atomic layer deposition, high-κ/III–V device integration, quantum/spin transport, nanostructures, and nanofabrication.

Linda P. B. Katehi (S'81–M'84–SM'89–F'95) is the Provost and Vice Chancellor for Academic Affairs at the University of Illinois at Urbana-Champaign and Professor of Electrical and Computer Engineering. Her research is focused on the development and characterization of 3-D integration and packaging of integrated circuits with particular emphasis on MEMS devices, high-Q evanescent mode filters and the theoretical and experimental study of planar circuits for hybrid-monolithic and monolithic oscillators, amplifiers, and mixer applications. Her work in this area has led to numerous national and international technical awards and to distinctions as an educator. She holds 13 U.S. patents and has authored more 600 papers published in refereed journals and symposia proceedings as well as nine book chapters.

Prof. Katehi is a member of the National Academy of Engineering, the Nominations Committee for the National Medal of Technology, the Kauffman National Panel for Entrepreneurship, the National Science Foundation (NSF) Advisory Committee to the Engineering Directorate, and numerous other engineering and scientific committees.

Saeed Mohammadi (S'89–M'92–SM'02) received the Ph.D. degree in electrical engineering from the University of Michigan, Ann Arbor, in 2000.

He is currently an Associate Professor of Electrical and Computer Engineering at Purdue University, West Lafayette, IN. His group is involved in research in RF devices and circuits, RF integration, and nanoelectronic technology. He has published more than 90 journal and refereed conference papers in these areas.

Dr. Mohammadi was an Associate Editor for IEEE MICROWAVE AND WIRELESS COMPONENTS LETTERS in 2006–2007.